Journal of Materials Chemistry A

Push-pull architecture eliminates chain length effects on exciton dissociation

Journal:	*Journal of Materials Chemistry A*
Manuscript ID	TA-ART-06-2018-005782.R1
Article Type:	Paper
Date Submitted by the Author:	07-Sep-2018
Complete List of Authors:	Aplan, Melissa; The Pennsylvania State University, Chemical Engineering Lee, Youngmin; The Pennsylvania State University, Chemical Engineering Wilkie, Carly; The Pennsylvania State University, Chemical Engineering Wang, Qing; The Pennsylvania State University, Materials Science and Engineering Gomez, Enrique; The Pennsylvania State University, Chemical Engineering

Push-pull architecture eliminates chain length effects on exciton dissociation

Melissa P. Aplan,[a] Youngmin Lee,[a] Carly A. Wilkie,[a] Qing Wang,[b] and Enrique D. Gomez[a,b,c]*

[a]*Department of Chemical Engineering, The Pennsylvania State University, University Park, PA 16802 USA.*
[b]*Department of Materials Science, The Pennsylvania State University, University Park, PA 16802 USA*
[c]*Materials Research Institute, The Pennsylvania State University, University Park, PA 16802 USA*

Electronic Supplementary Information (ESI) available: See DOI: 10.1039/x0xx00000x

*E-mail: edg12@psu.edu

Abstract

Recent development of small molecule non-fullerene acceptors have led to remarkable performance when incorporated in organic photovoltaic devices. These non-fullerene acceptors typically consist of about 10 aromatic rings arranged in an alternating electron-rich/electron-deficient architecture reminiscent of push-pull polymers, making them "push-pull oligomers". Without the extended conjugation length of a polymer, it is perhaps surprising that devices incorporating oligomeric non-fullerene acceptors perform so well. To investigate exciton dissociation as a function of chain length, a series of donor-acceptor block copolymers consisting of a conjugated homopolymer electron donor, poly(3-hexylthiophene-2,5-diyl) (P3HT), covalently linked to a push-pull polymer electron acceptor, poly-((2,5-dihexylphenylene)-1,4-diyl-alt-[4,7-bis(3-hexylthiophen-5-yl)-2,1,3-benzothiadiazole]-2',2"-diyl) (PPT6BT), was synthesized. By adjusting synthetic parameters, the chain length of each block is selectively tuned. The block copolymers are dissolved as isolated chains in dilute solutions and intramolecular charge transfer is quantified. When the P3HT block is very short (< 3 nm), charge transfer is inhibited. Nevertheless, efficient charge transfer is observed for PPT6BT block lengths ranging from essentially a single repeat unit to 16 nm. This indicates that the polarized nature and charge transfer character of excited states generated along push-pull polymers facilitates exciton dissociation.

Introduction

Performance of organic photovoltaic (OPV) devices has increased rapidly, such that power conversion efficiencies of single-junction cells exceed 13% and tandem cells are over 17%.[1-6] Historically, the active layer of top-performing OPV devices has been composed of a polymer electron donor, made up of alternating electron-rich (push) and electron-deficient (pull) moieties, blended with a solubilized fullerene derivative electron acceptor.[7-14] While push-pull polymers remain unrivaled as electron donors, recently, non-fullerene acceptors have rapidly emerged as champion materials; efficiencies of devices incorporating non-fullerene acceptors now surpass efficiencies of polymer/fullerene devices.[1-5]

In addition to electron donors, n-type push-pull polymers are also promising materials for non-fullerene electron acceptors.[15-24] Non-fullerene OPV devices incorporating an alternating naphthalene diimide-bithiophene polymer as the electron acceptor have achieved efficiencies approaching 10%.[15, 24] Nevertheless, the top-performing non-fullerene OPVs incorporate "small molecule" acceptors. The chemical structure of these small molecule acceptors typically includes linear chains of aromatic moieties (~ 10 aromatic rings) arranged in alternating electron-rich/electron-deficient pattern reminiscent of push-pull polymers. [1-5, 25-35] It is surprising that OPV devices incorporating these "push-pull oligomer" non-fullerene acceptors perform well despite the electron acceptor not having the extended conjugation length of a polymer.

When blended with another material, polymer chain length will influence morphological properties including crystallinity, crystal packing, and domain spacing. As a result, chain length can have a profound effect on exciton diffusion, charge transport, and thus, overall photovoltaic device performance.[36-46] For example, using fluorescence quenching experiments to measure vertical exciton diffusion (normal to the substrate) within P3HT films, the exciton diffusion coefficient was found to be an order of magnitude greater within high molecular weight P3HT (76 kg mol^{-1}) than within lower molecular weight P3HT (14 kg mol^{-1}), ~10^{-3} cm^2 s^{-1} versus ~10^{-4} cm^2 s^{-1}. respectively.[47] This was attributed to greater disorder in crystal texturing within the high molecular weight film, such that more polymer chains were oriented face-on with respect to the substrate. Thus, vertical exciton diffusion is potentially enhanced due to more tight chain

packing in the out-of-plane direction. Alternatively, increasing molecular weight could enhance exciton diffusion by providing intramolecular pathways for transport.[48] Thus, it is unclear whether the difference in exciton diffusion is due to different polymer chain lengths or if it is purely due to differences in film morphology.

Chain length can also influence the optoelectronic properties of a conjugated polymer. For example, oligothiophenes do not have the same optical bandgap as high molecular weight P3HT, indicating that P3HT oligomers have a shorter effective conjugation length than the polymer.[44, 45, 49] This result holds when the materials are dissolved in solution and cast into a film. P3HT is a conjugated homopolymer, consisting of repeating electron-rich thiophene units, and OPV devices incorporating a monodisperse P3HT oligomer (number of repeat units, n = 16) electron donor blended with [6,6]-phenyl-C61 butyric acid methyl ester ($PC_{61}BM$) fullerene electron acceptor perform significantly worse than devices incorporating high molecular weight P3HT blended with $PC_{61}BM$ (< 1% vs 5%).[50, 51] Interestingly, OPV devices incorporating an oligothiophene (n = 7) blended with $PC_{61}BM$ can achieve efficiencies of 5.1% when the oligothiophene is functionalized at the ends with electron withdrawing cyanoacrylate groups.[52] Functionalizing the oligothiophene with electron-deficient groups introduces the push-pull motif common in the polymer donors and non-fullerene acceptors used in top-performing OPV devices.

Here, we use conjugated block copolymers to examine the effect of chain length on exciton dissociation in both conjugated homopolymers and push-pull alternating copolymers. The block copolymers are studied as isolated chains in dilute solutions, decoupling exciton dissociation from the morphological effects present in a polymer film. In the past, covalently linked donor-acceptor dyads have been used extensively to examine intramolecular electron transfer processes.[53-65] These materials are typically composed of small molecule electron donors and acceptors joined by a saturated hydrocarbon linking group that limits intramolecular electronic coupling. Using block copolymers composed of conjugated donors and acceptors gives us the unique ability to examine intramolecular charge transfer as a function of donor and acceptor conjugation length.

The block copolymers studied consist of a P3HT conjugated homopolymer electron donor covalently linked to a push-pull polymer electron acceptor, poly-((2,5-dihexylphenylene)-1,4-diyl-alt-[4,7-bis(3-hexylthiophen-5-yl)-2,1,3-benzothiadiazole]-2',2"-diyl) (PPT6BT), yielding P3HT-*b*-PPT6BT. By adjusting the synthetic procedure for the block copolymers, the chain length of each block is systematically tuned. The block copolymers are designed to decouple energy transfer and charge transfer occurring within individual block copolymer chains, allowing us to monitor each process individually. Intramolecular charge transfer is quantified and chain length effects on exciton dissociation are examined in conjugated homopolymers and push-pull polymers. Results suggest a push-pull architecture decreases the requirement of an extended conjugation length for efficient exciton dissociation to a charge transfer state.

Results and discussion

Material design

The block copolymers studied in this work consist of a conjugated homopolymer (P3HT) covalently linked to a push-pull polymer (PPT6BT) and are based on block copolymers that can achieve over 3% power conversion efficiencies when implemented as the active layer in solar cells[66, 67]. Molecular structures are shown in Fig. 1. Using two similar block copolymers, poly(3-hexylthiophene-2,5-diyl)-*block*-poly-((9-(9-heptadecanyl)-9H-carbazole)-1,4-diyl-alt-[4,7-bis(3-hexylthiophen-5-yl)-2,1,3-benzothiadiazole]-2',2"-diyl) (P3HT-*b*-PCT6BT) and poly(3-hexylthiophene-2,5-diyl)-*block*-poly-((9,9-dioctylfluorene)-2,7-diyl-alt-[4,7-bis(3-hexylthiophen-5-yl)-2,1,3-benzothiadiazole]-2',2"-diyl) (P3HT-*b*-PFT6BT), we have previously demonstrated that small perturbations to the molecular structure can have a significant impact on intramolecular charge transfer.[68] In P3HT-*b*-PCT6BT, where a carbazole moiety is used as the electron-rich unit of the push-pull polymer electron acceptor, effectively no charge transfer is observed in chloroform solution ($\varepsilon = 4.81$). The driving force for exciton dissociation via hole transfer, defined as the energy difference between the excited state of the acceptor and charge transfer (CT) state, is 0.25 eV. The energy of the singlet exciton is the optical bandgap measured by the absorption onset and the CT state energy is

calculated using constrained density-functional theory. Moderately efficient charge transfer is observed in P3HT-*b*-PFT6BT, which incorporates a relatively less electron-rich fluorene moiety in the acceptor. The driving force for hole transfer is increased to 0.29 eV. Approximately 10% of excitons generated along P3HT-*b*-PFT6BT block copolymer chains dissociate to a charge transfer state transfer state.[68] In P3HT-*b*-PPT6BT, we decrease the electron donating ability of the electron-rich unit in the acceptor further by incorporating a phenyl ring as the electron-rich unit of the acceptor block. Thus, the driving force with chloroform as the solvent is increased further to 0.37 eV.

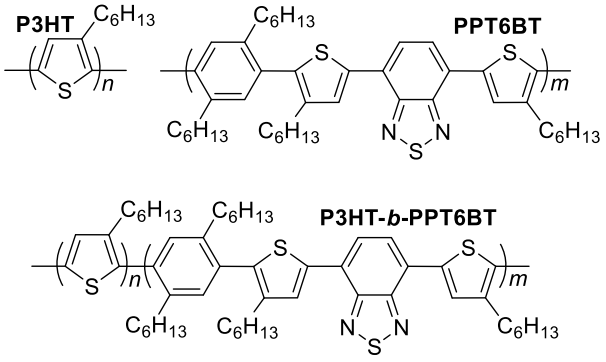

Fig. 1 Chemical structures of P3HT, PPT6BT, and P3HT-*b*-PPT6BT. P3HT is a homopolymer composed of repeating electron-rich thiophene units. PPT6BT is an alternating push-pull copolymer composed of alternating electron-rich phenyl units and electron-deficient dithienylbenzothiadiazole (T6BT) units.

Additionally, P3HT-*b*-PPT6BT was carefully designed to decouple energy transfer and charge transfer such that these processes could be monitored independently. In solution, energy transfer occurs predominately from P3HT to PPT6BT. The rate of energy transfer from a donor to an acceptor is directly proportional to the degree of spectral overlap, quantified by the overlap integral.[69] The overlap integral for energy transfer from P3HT to PPT6BT is 5.9 x 10^{13} $M^{-1}cm^{-1}nm^4$ while the overlap integral for energy transfer from PPT6BT to P3HT is 5.9 x 10^{11} $M^{-1}cm^{-1}nm^4$ (Fig. S1; ESI). Because the overlap integral for energy transfer from P3HT to PPT6BT is two orders of magnitude greater than the overlap integral for energy transfer from PPT6BT to P3HT, we assume the latter is negligible. Furthermore, in solution, charge transfer is expected to occur primarily via hole transfer from PPT6BT to P3HT. We have previously demonstrated that the electron-rich unit of the acceptor block disrupts electronic coupling between the

strong electron donor (P3HT) and highly electron-withdrawing benzothiadiazole, preventing excited state electron transfer from P3HT to the acceptor almost completely.[68, 70] Any charge transfer observed in P3HT-*b*-PPT6BT chains is assumed to be the result of hole transfer from PPT6BT to P3HT. Thus, in isolated P3HT-*b*-PPT6BT chains, we measure energy transfer from donor to acceptor and charge transfer from acceptor to donor.

Synthesis and chain length characterization

Block copolymers were synthesized in two steps as reported previously.[71] First, a P3HT macroreagent was synthesized using a Kumada catalyst transfer polymerization (KCTP) reaction, resulting in end-functionalized P3HT. The PPT6BT block was added on in a chain extension reaction using Suzuki polycondensation. Successful chain extension and block copolymer synthesis is confirmed by unimodal gel permeation chromatography (GPC) absorbance traces (recorded at 420 nm, where P3HT absorbs) of the block copolymer that are shifted to a higher molecular weight (lower retention time) relative to the P3HT macroreagent used (Fig. 2a).

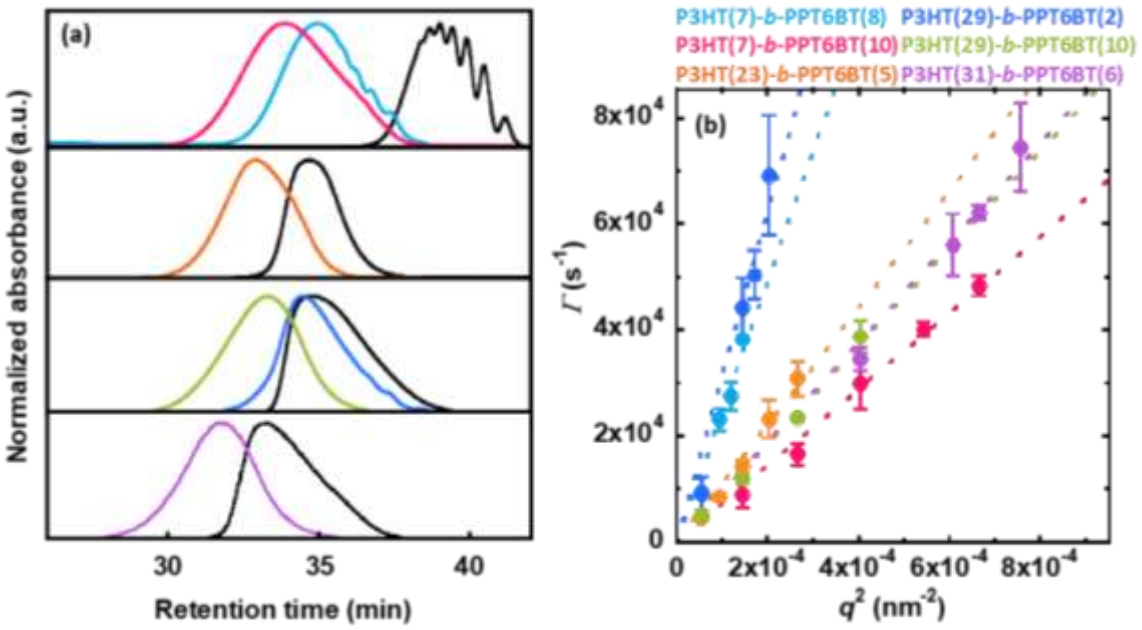

Fig. 2 Molecular weight and size characterization of synthesized block copolymers. (a) GPC traces of the block copolymers (colored traces) overlaid with the P3HT macroreagent used (black traces). Block copolymer synthesis is confirmed by a unimodal molecular weight distribution and shift away from the macroreagent to lower retention times. All traces are normalized to one for clarity. (b) Dynamic light scattering results plotted as the autocorrelation function decay rate (Γ) as a function of the scattering vector (q) squared.

By adjusting synthetic parameters, the chain length of each block can be systematically tuned. KCTP is known to follow a controlled chain-growth polymerization mechanism; the number-average degree of polymerization (X_n) can be tuned by altering the molar ratio of monomer to initiator (catalyst).[72-76] By adjusting this ratio, P3HT macroreagents were synthesized with M_n varying from 1100 to 5100 g mol^{-1}. Molecular weight is characterized using NMR end-group analysis to obtain absolute M_n of synthesized P3HT samples. Once we obtain an accurate value for M_n, the average contour length can be calculated simply as the product of X_n (M_n divided by repeat unit mass) and the monomer length (0.4 nm).[77] Thus, we synthesize P3HT samples with average contour lengths (L_{P3HT}) ranging from 2.6 to 12.2 nm. Different samples of P3HT are referred to as P3HT(x), where x denotes the X_n of the sample. In addition to a high catalyst loading, the acetone fraction was collected during Soxhlet purification to ensure a low molecular weight for the P3HT(7) macroreagent.

Suzuki polycondensation follows a step-growth mechanism, making control of the molecular weight challenging. According to Carothers equation, the maximum attainable X_n can be limited by using

an asymmetric molar ratio of the two condensation monomers. By adjusting this ratio in the chain-extension reaction, block copolymers were synthesized with PPT6BT blocks varying from 1500 to 7800 g mol^{-1}. Because M_n for the P3HT block is known, we can again use NMR to calculate M_n of the PPT6BT block in each block copolymer sample. We first calculate the weight composition of the block copolymer using signals that are unique to P3HT and PPT6BT. The M_n of the PPT6BT block can then be calculated using the absolute M_n previously calculated by end-group analysis of the corresponding P3HT macroreagent. Using this M_n value and the monomer width (1.5 nm), the contour length is calculated. Block copolymers used in this study have average PPT6BT contour lengths (L_{PPT6BT}) ranging from 3.2 to 15.4 nm. Molecular weight characterization is presented in Table 1; synthetic details can be found in Table S1 and Table S2. The block copolymers are named according to P3HT(x)-*b*-PPT6BT(y) where x is the X_n of the P3HT block and y is the X_n of the PPT6BT block.

Table 1 Molecular weight and size characterization of block copolymers

	P3HT M_n[a] (g mol^{-1})	P3HT L (nm)	PPT6BT M_n (g mol^{-1})	PPT6BT L (nm)	P3HT-*b*-PPT6BT M_n (g mol^{-1})	P3HT-*b*-PPT6BT Đ	Measured R_h[b] (nm)	Expected R_h[c] (nm)
P3HT(7)-*b*-PPT6BT(8)	1100	2.6	5500	11.6	6600	1.4	2	2
P3HT(7)-*b*-PPT6BT(10)	1100	2.6	7300	15.4	8400	1.6	6	2
P3HT(23)-*b*-PPT6BT(5)	3900	9.4	3700	7.8	7600	1.2	4	2
P3HT(29)-*b*-PPT6BT(2)	4800	11.5	1500	3.2	6300	1.4	2	2
P3HT(29)-*b*-PPT6BT(10)	4800	11.5	7300	15.4	12100	1.4	5	3
P3HT(31)-*b*-PPT6BT(6)	5100	12.2	4200	8.9	9300	1.3	5	3

[a] ^{1}H NMR; [b] DLS; [c] freely-rotating chain model

Block copolymers were dissolved in chloroform at ~ 1 mg L^{-1}. At such low concentrations, there are no intermolecular interactions or aggregation of polymer chains. This is confirmed by multiangle dynamic light scattering (DLS) profiles with unimodal particle size distributions where we measure apparent hydrodynamic radii (R_h) consistent with isolated semiflexible chains (Fig. 2b, Fig. S2; ESI).

Diffusion coefficients of the particles in chloroform solution were measured by plotting the mean decay rate of the autocorrelation function (Γ) versus the scattering vector (q) squared. The Stokes-Einstein equation was used to calculate the apparent hydrodynamic radius from the diffusion coefficient.

DLS also serves to support our calculations for L_{P3HT} and L_{PPT6BT}. As the molecular weight of the block copolymers increases from 6600 to 12100 g mol^{-1}, the measured R_h values increase from 2 to 5 nm. To calculate expected R_h values, we first calculate persistence lengths of 3 nm for P3HT and 4.4 nm for and PPT6BT in the freely-rotating chain limit as previously reported; this approach has been validated by comparing predicted values of P3HT and values from neutron scattering of P3HT in solution.[77, 78] Using the measured contour length and calculated persistence length values, we then calculate the radius of gyration (R_g) for a semiflexible polymer according to the freely-rotating chain model. To calculate an expected R_h from R_g, we use R_g/R_h = 1.73 that is expected for linear chains with significant dispersity in molecular weight.[79] In calculating expected R_h we assume that chloroform is a theta solvent for both P3HT and PPT6BT. Despite this, measured and expected R_h are in reasonable agreement, even though values measured through DLS are typically larger by 1 or 2 nanometers (Table 1). Although one possibility is that the persistence lengths are underestimated, R_h depends weakly on the persistence length for the low molecular weights used in this study. Instead, we hypothesize that chloroform is a good solvent for P3HT-*b*-PPT6BT, such that chains are more extended than conformations for unperturbed semiflexible chains.

Steady state absorbance and emission spectra from all block copolymers are shown in Fig. 3. Linear combinations of P3HT and PPT6BT homopolymer absorbance and emission spectra nicely describe the block copolymer absorbance and emission spectra. The block copolymer spectra are deconvoluted to determine the individual contributions of each block to both absorbance and emission. As previously reported, we quantify 1) the fraction of P3HT excited states that undergo energy transfer to the PPT6BT block (f_Q), and 2) the fraction of excitons generated on the block copolymer that dissociate to a charge transfer state, or the CT state yield, simply by comparing the quantum yield of the individual blocks with that of the homopolymers; we briefly describe this procedure in the Supplementary Information (Fig. S3; ESI).[68]

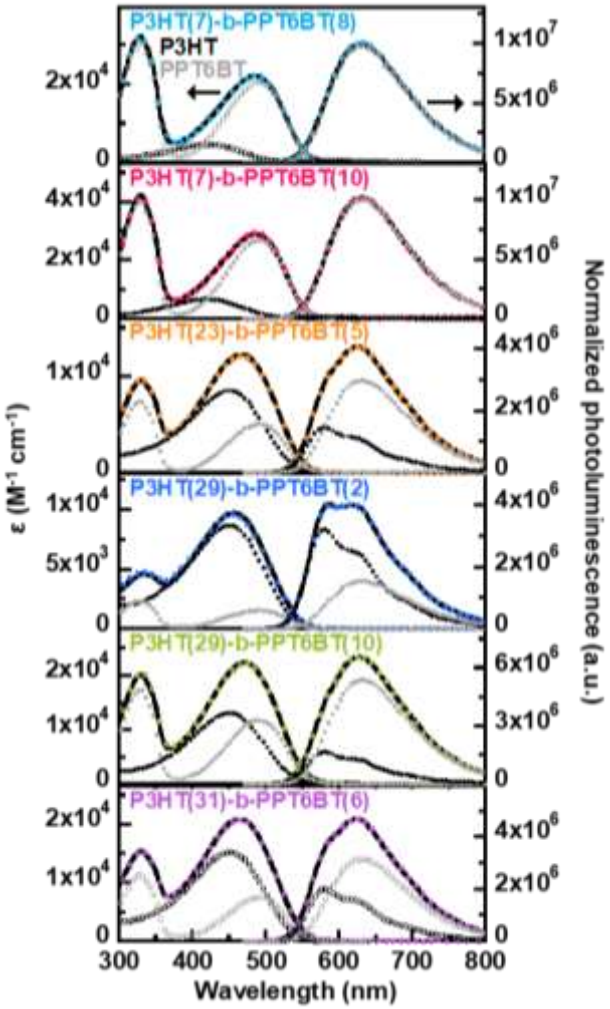

Fig. 3 Steady state absorbance as molar absorptivity, ε and photoluminescence spectra of dilute polymer solutions. Filled-in colored markers are the block copolymers, unfilled black markers are P3HT homopolymer, and unfilled gray markers are PPT6BT homopolymer. A linear combination of the homopolymer spectra (solid black lines) describes the block copolymer spectra. The homopolymer spectra are scaled by their contribution to the linear combination.

Exciton diffusion as a function of chain length

The strong dependence of f_Q on the P3HT contour length is used to estimate an exciton diffusion length along P3HT chains in chloroform solution (Fig. 4). f_Q data is fit using a one-dimensional diffusion equation.[80-82] Energy transfer is believed to occur by Förster resonance energy transfer and is therefore used to describe the boundary condition at the P3HT-PPT6BT donor-acceptor interface.[69] Previous studies have modeled exciton diffusion along P3HT chains linked to a fullerene electron acceptor moiety in solution, but cannot distinguish between energy transfer and charge transfer as the quenching mechanism at the

donor-acceptor interface.[80] The block copolymers in this study were designed to monitor energy transfer and charge transfer independently, allowing for a more accurate model. We calculate an exciton diffusion length along the P3HT backbone of 2.5 nm.

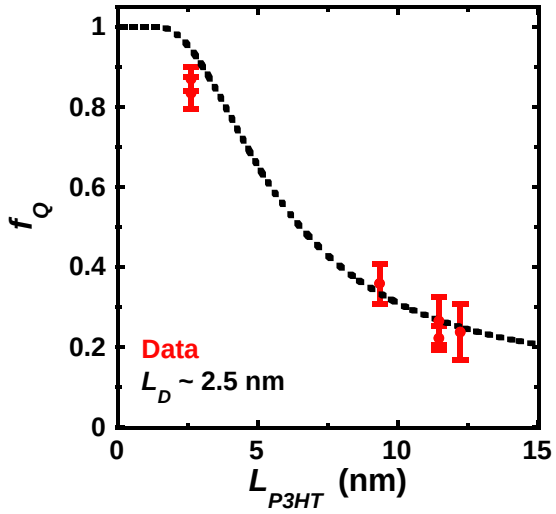

Fig. 4 P3HT quench fraction (f_Q) as a function of P3HT contour length. Red markers correspond to data for the block copolymers and the dotted black line is the diffusion model assuming all P3HT quenching at the donor-acceptor interface is due to FRET.

Our results suggest that dihedral disorder in solution places bounds on exciton diffusion and localizes excited states to 2.5 nm segments along P3HT chains. There is evidence that significant torsion along the backbone of conjugated polymers leads to localization of excited states.[83-85] Furthermore, theoretical calculations have demonstrated that charge carriers are able to move relatively fast along straight segments of a polymer chain until reaching a sharp twist where they are deeply trapped by the vanishing hopping integral.[86] There is evidence that, on very short time scales, structural disorder can broaden the distribution of exciton hopping rates and may initially enhance exciton diffusion; excitons preferentially hop downhill in energy. Nevertheless, at long time scales, after excitons have relaxed to low energy molecular subunits, structural disorder serves only to reduce overall exciton transport.[87] Thus, at steady state, we assume exciton motion along a conjugated polymer chain is localized by torsion in a similar manner as electrons or holes. Under this assumption, the dihedral potential suggests that every 2.5 nm there will be a 45° twist in the chain for P3HT chains well dispersed in chloroform. At 45°, the matrix hopping

element is approximately 70% of its maximum value and decreases rapidly to almost 0 as the dihedral angle approaches 90°.[77, 86, 88] This suggests that a 45° twist in the chain creates a significant enough barrier to disrupt transport and confine excitons to approximately 2.5 nm segments along the P3HT backbone.

This interpretation is consistent with previous studies examining exciton diffusion in P3HT films. In the solid state, P3HT chains crystallize; the thiophene rings π-stack and the polymer chains become increasingly planar. As crystalline order is increased by thermal annealing, exciton hopping rates and the exciton diffusion length, measured by photoluminescence quenching experiments, also increase. The exciton diffusion length increases from 3 nm in a low crystallinity, as-cast film to 7 nm in a highly crystalline film after chains are recrystallized from the melt.[89] In addition, earlier theoretical work suggests a dihedral angle greater than 40° is sufficient to effectively break conjugation and disrupt the electronic properties of polythiophene.[90]

These results suggest that in designing non-fullerene acceptors for OPVs, chain planarity should be considered. There is evidence to suggest that in some top-performing polymer/fullerene systems, exciton diffusion is not a significant factor in the photocurrent generation mechanism.[91-96] This could be due to the miscibility between fullerene and many amorphous conjugated polymers. When blended together, these materials form intimately mixed phases, unlike the pure donor-acceptor domains often illustrated. Thus, when an excited state is generated along the polymer chain, it is very likely to be generated near a donor-acceptor interface; no diffusion is required. This could differ in non-fullerene solar cells. As the degree of polymerization increases, the loss in entropy of mixing makes miscibility less likely.[97] Assuming moderate molecular weights or greater, polymer blends will almost always phase separate. An n-type conjugated polymer acceptor will almost certainly not form an intimately mixed phase with a conjugated polymer donor. Furthermore, depending on the interaction energy of a particular oligomeric non-fullerene acceptor/polymer donor pair, blend morphology may consist of an intimately mixed phase or strongly segregated, pure domains. Pure domains of electron donor and/or acceptor are suspected to be necessary to achieve high performance.[68, 94, 98] Thus, exciton diffusion will likely contribute to the mechanism of photocurrent generation in non-fullerene solar cells. Our results suggest that exciton diffusion is disrupted

by significant twisting of aromatic rings along the backbone. Polymers and oligomers that have more rigid, planar backbones due to molecular design or intermolecular aggregation will likely facilitate longer exciton diffusion lengths.

Exciton dissociation as a function of chain length

Any quenching of excited states generated along either the P3HT block or the PPT6BT block not accounted for by energy transfer is assumed to be the result of intramolecular charge transfer and is therefore proportional to the CT state yield. CT state yield as a function of L_{P3HT} is presented in Fig. 5a. The black dashed line starting at 0% that quickly saturates to about 20% serves as a guide to the eye. When P3HT chains are very short (~ 2.6 nm), the CT state yield is only around 5%. This suggests that confining charge transfer states along short P3HT chains introduces an energetic penalty that disrupts charge transfer.

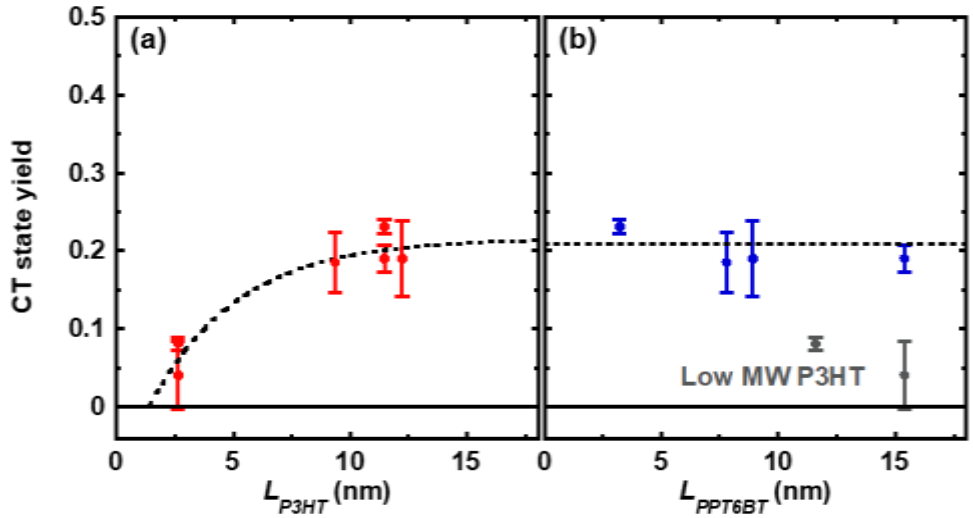

Fig. 5 CT state yield as a function of both P3HT and PPT6BT contour length. (a) As the contour length of P3HT chains increases, the CT state yield quickly rises and saturates at almost 20%. (b) Charge transfer is largely independent of PPT6BT contour length (blue markers), although it drops significantly when the P3HT block chain length is short (gray markers). The black lines in both plots serve as a guide to the eye.

Conversely, charge transfer is mostly independent of the PPT6BT average chain length (Fig. 5b). Again, the black dashed line serves as a guide to the eye. This result is unexpected. First, as the chains become longer, a drop in the CT state yield is expected due to limited access of excitons to the donor-acceptor junction. Nevertheless, the CT state yield remains at about 20% for the average L_{PPT6BT} ranging

from approximately 3 to 15 nm. This result is consistent with a very long exciton diffusion length, possibly greater than 15 nm, along the PPT6BT backbone. There is evidence that push-pull polymers in solution can support relatively long exciton diffusion lengths, possibly as high as 10-15 nm, particularly when excited above the bandgap.[99-101] Confirmation of long exciton diffusion lengths will require studies of high molecular weight PPT6BT blocks that do not aggregate or chain-fold, to prevent the introduction of additional donor-acceptor contacts beyond the block junction.

Furthermore, based on results shown in Fig. 5a, a decrease in CT state yield might be expected as the average chain length of PPT6BT decreases. Our results demonstrate that when PPT6BT chains are very short ($L_{PPT6BT} \approx 3$ nm), confinement effects are not observed and charge transfer remains very efficient with a measured CT state yield of 23%. In fact, our results suggest that even a single repeat unit of PPT6BT does not result in an energetic penalty due to confinement of the charge transfer state. This can be understood by considering the statistical nature of polymers and the step-growth mechanism used to synthesize PPT6BT. In P3HT(29)-*b*-PPT6BT(2), although the average PPT6BT X_n is 2, approximately 40% of P3HT(29)-*b*-PPT6BT(2) chains are likely to be functionalized by a single PPT6BT repeat unit, referred to as P3HT-PT6BT (see ESI for details).[102] If these P3HT-PT6BT chains did not result in efficient exciton dissociation, we would expect a significant drop in the CT state yield and a measured value as low as 12% (Table S2; ESI). Nevertheless, the CT state yield measured for P3HT(29)-*b*-PPT6BT(2) is close to 23%. Thus, confinement effects are not observed even with a single push-pull repeat unit.

It has been shown that excited states generated on push-pull polymers are polarized and have significant charge transfer character.[99, 103-108] In a recent study comparing optoelectronic properties of conjugated homopolymers and push-pull polymers, it was found that the energy gap reduction with increasing oligomer chain length was much less pronounced in push-pull polymers.[99] In conjugated homopolymers such as P3HT, it appears that intramolecular delocalization is required (*i.e.*, chain lengths greater than 20 repeat units) to promote efficient exciton dissociation to a charge transfer state. Electronically different building blocks of push-pull polymers such as PPT6BT lead to polarization of

excited states along the backbone. As a consequence, and as our results show, an extended conjugation length is not necessary for efficient exciton dissociation to charge transfer states.

Oligomeric non-fullerene acceptors used in high-performance OPV devices consist of roughly 10 aromatic rings arranged in an alternating electron-rich/electron-deficient pattern. Their architecture is reminiscent of low molecular weight push-pull polymers, making them push-pull oligomers. In P3HT-*b*-PPT6BT, when the PPT6BT block is very short, approximately 3.2 nm on average but with a significant population of single repeat units, charge transfer appears to be just as efficient as when the chains are about 15 nm long. This suggests that the push-pull architecture for active layer materials can promote exciton dissociation to charge transfer states even when the conjugation length is limited. While this design principle is particularly relevant to push-pull oligomers that are currently being developed, we presume this rule is universal and can guide the design of any donor or acceptor material. This implies that the push-pull motif for new active layer materials is a crucial design criterion to achieve maximum photovoltages in devices, where the energy of the singlet excited state is nearly degenerate to that of the charge transfer state.

Furthermore, our results suggest a push-pull architecture may relax morphological requirements for achieving efficient photovoltaic performance. There is significant evidence to suggest that in polymer donor/fullerene acceptor systems, aggregation of fullerene into pure domains plays a critical role in charge generation.[91, 93, 94, 96, 109-111] This suggests that in devices incorporating fullerene, an electron acceptor not incorporating a push-pull architecture and with limited intramolecular delocalization, intermolecular delocalization can promote exciton dissociation. Thus, in homopolymer or fullerene materials that do not incorporate a push-pull architecture, significant intra or intermolecular delocalization is necessary to achieve efficient photovoltaic performance. In contrast, our results demonstrate that the push-pull architecture decreases the requirement of significant intramolecular delocalization to achieve efficient exciton dissociation. This in turn may also relax the morphological requirement of aggregation into pure domains and significant intermolecular delocalization in systems where both electron donor and acceptor incorporate a push-pull architecture.

Conclusions

Using conjugated block copolymers composed of a conjugated homopolymer electron donor covalently linked to a push-pull polymer electron acceptor, we examine the effect of polymer chain length on exciton diffusion and dissociation. An exciton diffusion length of ~ 2.5 nm is calculated for P3HT chains in chloroform solution. This corresponds to the approximate distance along the chain an exciton can travel before reaching a dihedral angle of 45°. Thus, a sharp twist in the chain disrupts exciton transport and more planar materials may facilitate longer exciton diffusion lengths.

By quantifying intramolecular charge transfer as a function of the P3HT and PPT6BT block average contour lengths, fundamental differences between conjugated homopolymers and push-pull polymers are investigated. Our results demonstrate that in conjugated homopolymers, such as P3HT, a chain length greater than 3 nm is required for efficient exciton dissociation. Below this contour length, confinement of the charge transfer state wave function introduces an energetic penalty and inhibits efficient charge transfer. In push-pull polymers, such as PPT6BT, efficient charge transfer is observed even with chain lengths that are less than 3 nm on average. We suspect this is facilitated by polarized excited states along a polymer chain composed of alternating electron-rich/electron-deficient units. As a consequence, the push-pull character eliminates chain length effects on exciton dissociation and enables single-site exciton dissociation to charge transfer states.

Experimental

Polymer synthesis

P3HT was synthesized using typical Kumada catalyst transfer polymerization reaction conditions according to a previously reported procedure.[71] The molar ratio of monomer/catalyst was adjusted to tune P3HT molecular weight. Block copolymers were synthesized using the end-functionalized P3HT as a macroreagent; the PPT6BT block was added on using a Suzuki polycondensation according to a previously

reported procedure.[71] PPT6BT homopolymer was synthesized using the same procedure as the block copolymers, omitting P3HT from the reaction.

P3HT(7), P3HT(29), P3HT(23), P3HT(31): Yields: ~ 700 mg, ~ 50%. ^{1}H NMR (850 MHz, $CDCl_3$, δ): 6.96 (1H), 2.78 (2H), 1.69 (2H), 1.42 (2H), 1.33 (4H), 0.90 (3H)

PPT6BT: Yield: 238 mg, 89%. ^{1}H NMR (850 MHz, $CDCl_3$, δ): 8.08 (2H), 7.88 (2H), 7.25 (2H), 2.60 (4H), 2.49 (4H), 1.64 (4H), 1.53 (4H), 1.24 (24H), 0.87 (6H), 0.80 (6H).

P3HT(7)-b-PPT6BT(8), P3HT(7)-b-PPT6BT(10), P3HT(23)-b-PPT6BT(5), P3HT(29)-b-PPT6BT(2), P3HT(29)-b-PPT6BT(10), P3HT(31)-b-PPT6BT(6): Yields: ~ 100-200 mg, ~ 60-80%. ^{1}H NMR (360 or 500 MHz, $CDCl_3$, δ): 8.08, 7.88, 7.25, 6.96, 2.78, 2.60, 2.49, 1.69, 1.42, 133-1.22, 0.90, 0.80

Gel permeation chromatography (GPC)

Chain extension and molar mass distributions were determined using an Agilent Technologies gel permeation chromatograph (ResiPore 300 x 7.5 mm column, Agilent 1260) equipped with multiwavelength (MWD) and refractive index (RID) detectors. Chlorobenzene was used as the mobile phase at 40°C and a flow rate of 0.5 mL min^{-1}. Molar mass distributions were determined relative to polystyrene standards.

^{1}H nuclear magnetic resonance (NMR) spectroscopy

Number average molecular weight (M_n) and contour length (L) of each block were characterized using ^{1}H NMR analysis. NMR was performed on a Bruker 850 MHz instrument (Bruker Avance-III-850 MHz); all samples were prepared in deuterated chloroform. M_n of P3HT was calculated by end-group analysis using the signals at 2.78, 2.60, and 2.55 ppm, corresponding to the protons on the α-CH_2 of the thiophene rings within the chain, on the protonated chain end, and on the brominated chain end, respectively. M_n of the PPT6BT block was calculated using the peak ratios corresponding to P3HT (δ = 2.78, 6.96 ppm) and PPT6BT (δ = 2.59, 2.49, 7.94, 8.14, 7.31 ppm) to obtain the relative weight fractions. The M_n of PPT6BT was then calculated using the weight fraction and M_n of P3HT. The contour length of each block is calculated as the product of monomer width (P3HT ~ 0.4 nm[77], PPT6BT ~ 1.6 nm) and the number average degree of polymerization, X_n. ^{1}H NMR spectra are presented in Fig. S5.

Dynamic light scattering (DLS)

DLS measurements were performed on P3HT-b-PPT6BT in chloroform (dissolved at ~ 0.1 – 0.25 mg mL^{-1} in chloroform) at room temperature using a Brookhaven Instruments BI-200 SM static/dynamic light scattering system equipped with a 30 mW diode laser (λ=637 nm). Particle size distributions were determined at various scattering angles ranging from 30 to 150°. CONTIN[112] algorithm was used to calculated the mean decay rate (Γ) of the autocorrelation function. Diffusion coefficients of the particles in chloroform were obtained by plotting Γ versus the scattering vector (q) squared. Stokes-Einstein equation was used to calculate the hydrodynamic radius from the diffusion coefficient.

Absorbance and fluorescence spectroscopy

Polymer solutions were prepared at 1 mg mL^{-1} in chloroform and stirred overnight in an inert atmosphere to ensure full dissolution. Solutions were diluted to 1 μg mL^{-1}, loaded into 1 cm path length quartz cuvettes, sealed and removed from the glovebox for testing. Absorbance spectra were measured on an Agilent Technologies Cary 60 UV-vis. Fluorescence emission spectra were measured on a Photon Technology International QuantaMaster 300 fluorimeter. Quantum efficiency measurements were made by comparing absorbance and fluorescence spectra to a dye of known quantum efficiency, 4-(Dicyanomethylene)-2-methyl-6-(4-dimethylaminostyryl)-4H-pyran (Φ = 0.44 in ethanol). [69, 113]

Acknowledgements

Financial support from the Office of Naval Research under Grant N000141410532 is gratefully acknowledged. MA acknowledges assistance from Shreya Shetty for calculations of the persistence length of PPT6BT.

Conflicts of interest

The authors declare no competing interests.

References

1. W. Zhao, S. Li, H. Yao, S. Zhang, Y. Zhang, B. Yang and J. Hou, *J. Am. Chem. Soc.*, 2017, **139**, 7148-7151.
2. J. Sun, X. Ma, Z. Zhang, J. Yu, J. Zhou, X. Yin, L. Yang, R. Geng, R. Zhu, F. Zhang and W. Tang, *Adv. Mater.*, 2018, **30**, 1707150.
3. W. Li, L. Ye, S. Li, H. Yao, H. Ade and J. Hou, *Adv. Mater.*, 2018, **30**, 1707170.
4. L. Zuo, X. Shi, S. B. Jo, Y. Liu, F. Lin and A. K. Y. Jen, *Adv. Mater.*, 2018, **30**, 1706816.
5. X. Che, Y. Li, Y. Qu and S. R. Forrest, *Nat. Energy*, 2018, DOI: 10.1038/s41560-018-0134-z.
6. L. Meng, Y. Zhang, X. Wan, C. Li, X. Zhang, Y. Wang, X. Ke, Z. Xiao, L. Ding, R. Xia, H.-L. Yip, Y. Cao and Y. Chen, *Science*, 2018, DOI: 10.1126/science.aat2612.
7. N. Blouin, A. Michaud and M. Leclerc, *Adv. Mater.*, 2007, **19**, 2295.
8. Z. He, B. Xiao, F. Liu, H. Wu, Y. Yang, S. Xiao, C. Wang, T. P. Russell and Y. Cao, *Nat. Photonics*, 2015, **9**, 174.
9. J. Y. Kim, K. Lee, N. E. Coates, D. Moses, T.-Q. Nguyen, M. Dante and A. J. Heeger, *Science*, 2007, **317**, 222-225.
10. G. Li, V. Shrotriya, J. Huang, Y. Yao, T. Moriarty, K. Emery and Y. Yang, *Nat. Mater.*, 2005, **4**, 864.
11. G. Li, R. Zhu and Y. Yang, *Nat. Photonics*, 2012, **6**, 153.
12. Y. Liu, J. Zhao, Z. Li, C. Mu, W. Ma, H. Hu, K. Jiang, H. Lin, H. Ade and H. Yan, *Nat. Commun.*, 2014, **5**, 5293.
13. S. J. Lou, J. M. Szarko, T. Xu, L. Yu, T. J. Marks and L. X. Chen, *J. Am. Chem. Soc.*, 2011, **133**, 20661-20663.
14. S. H. Park, A. Roy, S. Beaupré, S. Cho, N. Coates, J. S. Moon, D. Moses, M. Leclerc, K. Lee and A. J. Heeger, *Nat. Photonics*, 2009, **3**, 297.
15. L. Gao, Z.-G. Zhang, L. Xue, J. Min, J. Zhang, Z. Wei and Y. Li, *Adv. Mater.*, 2016, **28**, 1884-1890.
16. Y.-J. Hwang, B. A. E. Courtright, A. S. Ferreira, S. H. Tolbert and S. A. Jenekhe, *Adv. Mater.*, 2015, **27**, 4578-4584.
17. Y.-J. Hwang, T. Earmme, B. A. E. Courtright, F. N. Eberle and S. A. Jenekhe, *J. Am. Chem. Soc.*, 2015, **137**, 4424-4434.
18. J. W. Jung, J. W. Jo, C.-C. Chueh, F. Liu, W. H. Jo, T. P. Russell and A. K. Y. Jen, *Adv. Mater.*, 2015, **27**, 3310-3317.
19. H. Kang, M. A. Uddin, C. Lee, K.-H. Kim, T. L. Nguyen, W. Lee, Y. Li, C. Wang, H. Y. Woo and B. J. Kim, *J. Am. Chem. Soc.*, 2015, **137**, 2359-2365.

20. T. Kim, J.-H. Kim, T. E. Kang, C. Lee, H. Kang, M. Shin, C. Wang, B. Ma, U. Jeong, T.-S. Kim and B. J. Kim, *Nat. Commun.*, 2015, **6**, 8547.
21. C. Lee, H. Kang, W. Lee, T. Kim, K.-H. Kim, H. Y. Woo, C. Wang and B. J. Kim, *Adv. Mater.*, 2015, **27**, 2466-2471.
22. G. Shi, J. Yuan, X. Huang, Y. Lu, Z. Liu, J. Peng, G. Ding, S. Shi, J. Sun, K. Lu, H.-Q. Wang and W. Ma, *J. Phys. Chem. C*, 2015, **119**, 25298-25306.
23. L. Ye, X. Jiao, M. Zhou, S. Zhang, H. Yao, W. Zhao, A. Xia, H. Ade and J. Hou, *Adv. Mater.*, 2015, **27**, 6046-6054.
24. B. Fan, L. Ying, Z. Wang, B. He, X.-F. Jiang, F. Huang and Y. Cao, *Energy Environ. Sci.*, 2017, **10**, 1243-1251.
25. D. Baran, R. S. Ashraf, D. A. Hanifi, M. Abdelsamie, N. Gasparini, J. A. Röhr, S. Holliday, A. Wadsworth, S. Lockett, M. Neophytou, C. J. M. Emmott, J. Nelson, C. J. Brabec, A. Amassian, A. Salleo, T. Kirchartz, J. R. Durrant and I. McCulloch, *Nat. Mater.*, 2016, **16**, 363.
26. H. Feng, N. Qiu, X. Wang, Y. Wang, B. Kan, X. Wan, M. Zhang, A. Xia, C. Li, F. Liu, H. Zhang and Y. Chen, *Chem. Mater.*, 2017, **29**, 7908-7917.
27. B. Guo, W. Li, X. Guo, X. Meng, W. Ma, M. Zhang and Y. Li, *Adv. Mater.*, 2017, **29**, 1702291-n/a.
28. S. Holliday, R. S. Ashraf, A. Wadsworth, D. Baran, S. A. Yousaf, C. B. Nielsen, C.-H. Tan, S. D. Dimitrov, Z. Shang, N. Gasparini, M. Alamoudi, F. Laquai, C. J. Brabec, A. Salleo, J. R. Durrant and I. McCulloch, *Nat. Commun.*, 2016, **7**, 11585.
29. O. K. Kwon, M. A. Uddin, J.-H. Park, S. K. Park, T. L. Nguyen, H. Y. Woo and S. Y. Park, *Adv. Mater.*, 2016, **28**, 910-916.
30. Y. Lin, F. Zhao, Q. He, L. Huo, Y. Wu, T. C. Parker, W. Ma, Y. Sun, C. Wang, D. Zhu, A. J. Heeger, S. R. Marder and X. Zhan, *J. Am. Chem. Soc.*, 2016, **138**, 4955-4961.
31. Y. Yang, Z.-G. Zhang, H. Bin, S. Chen, L. Gao, L. Xue, C. Yang and Y. Li, *J. Am. Chem. Soc.*, 2016, **138**, 15011-15018.
32. N. Zarrabi, D. M. Stoltzfus, P. L. Burn and P. E. Shaw, *J. Phys. Chem. C*, 2017, **121**, 18412-18422.
33. C. Zhan and J. Yao, *Chem. Mater.*, 2016, **28**, 1948-1964.
34. S. Zhang, L. Ye and J. Hou, *Adv. Energy Mater.*, 2016, **6**, 1502529-n/a.
35. W. Zhao, D. Qian, S. Zhang, S. Li, O. Inganäs, F. Gao and J. Hou, *Adv. Mater.*, 2016, **28**, 4734-4739.
36. J.-F. Chang, J. Clark, N. Zhao, H. Sirringhaus, D. W. Breiby, J. W. Andreasen, M. M. Nielsen, M. Giles, M. Heeney and I. McCulloch, *Phys. Rev. B*, 2006, **74**, 115318.

37. R. Di Pietro, T. Erdmann, N. Wang, X. Liu, D. Grafe, J. Lenz, J. Brandt, D. Kasemann, K. Leo, M. Al-Hussein, K. L. Gerasimov, D. Doblas, D. A. Ivanov, B. Voit, D. Neher and A. Kiriy, *J. Mater. Chem. C*, 2016, **4**, 10827-10838.
38. A. Gasperini and K. Sivula, *Macromolecules*, 2013, **46**, 9349-9358.
39. J. J. Intemann, K. Yao, H.-L. Yip, Y.-X. Xu, Y.-X. Li, P.-W. Liang, F.-Z. Ding, X. Li and A. K. Y. Jen, *Chem. Mater.*, 2013, **25**, 3188-3195.
40. R. J. Kline, M. D. McGehee, E. N. Kadnikova, J. Liu, J. M. J. Fréchet and M. F. Toney, *Macromolecules*, 2005, **38**, 3312-3319.
41. F. P. V. Koch, J. Rivnay, S. Foster, C. Müller, J. M. Downing, E. Buchaca-Domingo, P. Westacott, L. Yu, M. Yuan, M. Baklar, Z. Fei, C. Luscombe, M. A. McLachlan, M. Heeney, G. Rumbles, C. Silva, A. Salleo, J. Nelson, P. Smith and N. Stingelin, *Progress in Polymer Science*, 2013, **38**, 1978-1989.
42. S. Li, S. Wang, B. Zhang, F. Ye, H. Tang, Z. Chen and X. Yang, *Org. Electron.*, 2014, **15**, 414-427.
43. D. Spoltore, T. Vangerven, P. Verstappen, F. Piersimoni, S. Bertho, K. Vandewal, N. Van den Brande, M. Defour, B. Van Mele, A. De Sio, J. Parisi, L. Lutsen, D. Vanderzande, W. Maes and J. V. Manca, *Org. Electron.*, 2015, **21**, 160-170.
44. L. Zhang, N. S. Colella, B. P. Cherniawski, S. C. B. Mannsfeld and A. L. Briseno, *ACS Appl. Mater. Interfaces*, 2014, **6**, 5327-5343.
45. L. Zhang, N. S. Colella, F. Liu, S. Trahan, J. K. Baral, H. H. Winter, S. C. B. Mannsfeld and A. L. Briseno, *J. Am. Chem. Soc.*, 2013, **135**, 844-854.
46. F. Liu, D. Chen, C. Wang, K. Luo, W. Gu, A. L. Briseno, J. W. P. Hsu and T. P. Russell, *ACS Appl. Mater. Interfaces*, 2014, **6**, 19876-19887.
47. Z. Masri, A. Ruseckas, E. V. Emelianova, L. Wang, A. K. Bansal, A. Matheson, H. T. Lemke, M. M. Nielsen, H. Nguyen, O. Coulembier, P. Dubois, D. Beljonne and I. D. W. Samuel, *Adv. Energy Mater.*, 2013, **3**, 1445-1453.
48. W. Zhang, S. T. Milner and E. D. Gomez, *ACS Central Science*, 2018, **4**, 413-421.
49. J. L. Bredas, R. Silbey, D. S. Boudreaux and R. R. Chance, *J. Am. Chem. Soc.*, 1983, **105**, 6555-6559.
50. F. Di Maria, M. Gazzano, A. Zanelli, G. Gigli, A. Loiudice, A. Rizzo, M. Biasiucci, E. Salatelli, P. D' Angelo and G. Barbarella, *Macromolecules*, 2012, **45**, 8284-8291.
51. W. Ma, C. Yang, X. Gong, K. Lee and A. J. Heeger, *Adv. Funct. Mater.*, 2005, **15**, 1617-1622.
52. Y. Liu, X. Wan, F. Wang, J. Zhou, G. Long, J. Tian, J. You, Y. Yang and Y. Chen, *Adv. Energy Mater.*, 2011, **1**, 771-775.

53. G. L. Closs, L. T. Calcaterra, N. J. Green, K. W. Penfield and J. R. Miller, *J. Phys. Chem.*, 1986, **90**, 3673-3683.
54. I. Fujita, J. Fajer, C. K. Chang, C. B. Wang, M. A. Bergkamp and T. L. Netzel, *J. Phys. Chem.*, 1982, **86**, 3754-3759.
55. H. Heitele, P. Finckh, S. Weeren, F. Poellinger and M. E. Michel-Beyerle, *J. Phys. Chem.*, 1989, **93**, 5173-5179.
56. R. K. Huddleston and J. R. Miller, *J. Chem. Phys.*, 1983, **79**, 5337-5344.
57. N. S. Hush, M. N. Paddon-Row, E. Cotsaris, H. Oevering, J. W. Verhoeven and M. Heppener, *Chem. Phys. Lett.*, 1985, **117**, 8-11.
58. J. S. Lindsey, D. C. Mauzerall and H. Linschitz, *J. Am. Chem. Soc.*, 1983, **105**, 6528-6529.
59. R. A. Marcus, *J. Phys. Chem.*, 1963, **67**, 853-857.
60. J. R. Miller, L. T. Calcaterra and G. L. Closs, *J. Am. Chem. Soc.*, 1984, **106**, 3047-3049.
61. T. A. Moore, D. Gust, P. Mathis, J.-C. Mialocq, C. Chachaty, R. V. Bensasson, E. J. Land, D. Doizi, P. A. Liddell, W. R. Lehman, G. A. Nemeth and A. L. Moore, *Nature*, 1984, **307**, 630.
62. P. Pasman, J. W. Verhoeven and T. J. De Boer, *Chem. Phys. Lett.*, 1978, **59**, 381-385.
63. J. W. Verhoeven, T. Scherer, B. Wegewijs, R. M. Hermant, J. Jortner, M. Bixon, S. Depaemelaere and F. C. de Schryver, *Recl. Trav. Chim. Pays-Bas*, 1995, **114**, 443-448.
64. M. R. Wasielewski, M. P. Niemczyk, W. A. Svec and E. B. Pewitt, *J. Am. Chem. Soc.*, 1985, **107**, 5562-5563.
65. M. R. Wasielewski, M. P. Niemczyk, W. A. Svec and E. B. Pewitt, *J. Am. Chem. Soc.*, 1985, **107**, 1080-1082.
66. C. Guo, Y.-H. Lin, M. D. Witman, K. A. Smith, C. Wang, A. Hexemer, J. Strzalka, E. D. Gomez and R. Verduzco, *Nano Lett.*, 2013, **13**, 2957-2963.
67. Y. Lee and E. D. Gomez, *Macromolecules*, 2015, **48**, 7385-7395.
68. M. P. Aplan, C. Grieco, Y. Lee, J. M. Munro, B. Kuei, J. L. Gray, Z. D. Seibers, S. M. Kilbey, Q. Wang, I. Dabo, J. B. Asbury and E. D. Gomez, *Submitted to Advanced Functional Materials*, 2018.
69. J. R. Lakowicz, *Principles of Fluorescence Spectroscopy*, Springer US, New York, NY, USA, 2007.
70. C. Grieco, M. P. Aplan, A. Rimshaw, Y. Lee, T. P. Le, W. Zhang, Q. Wang, S. T. Milner, E. D. Gomez and J. B. Asbury, *J. Phys. Chem. C*, 2016, **120**, 6978-6988.
71. Y. Lee, M. P. Aplan, Z. D. Seibers, S. M. Kilbey, Q. Wang and E. D. Gomez, *J. Mater. Chem. A*, 2017, **5**, 20412-20421.
72. M. P. Aplan and E. D. Gomez, *Ind. Eng. Chem. Res.*, 2017, **56**, 7888-7901.

73. Z. J. Bryan and A. J. McNeil, *Chemical Science*, 2013, **4**, 1620-1624.
74. R. S. Loewe, S. M. Khersonsky and R. D. McCullough, *Adv. Mater.*, 1999, **11**, 250-253.
75. E. E. Sheina, J. Liu, M. C. Iovu, D. W. Laird and R. D. McCullough, *Macromolecules*, 2004, **37**, 3526-3528.
76. A. Yokoyama, R. Miyakoshi and T. Yokozawa, *Macromolecules*, 2004, **37**, 1169-1171.
77. W. Zhang, E. D. Gomez and S. T. Milner, *Macromolecules*, 2014, **47**, 6453-6461.
78. B. Kuei and E. D. Gomez, *Soft Matter*, 2017, **13**, 49-67.
79. W. Burchard, *Advances in Polymer Science*, 1983, **48**, 1-124.
80. A. T. Healy, B. W. Boudouris, C. D. Frisbie, M. A. Hillmyer and D. A. Blank, *J. Phys. Chem. Lett.*, 2013, **4**, 3445-3449.
81. R. R. Lunt, N. C. Giebink, A. A. Belak, J. B. Benziger and S. R. Forrest, *J. Appl. Phys.*, 2009, **105**, 053711.
82. O. Simpson, *Proceedings of the Royal Society of London. Series A. Mathematical and Physical Sciences*, 1957, **238**, 402-411.
83. K. F. Wong, M. S. Skaf, C.-Y. Yang, P. J. Rossky, B. Bagchi, D. Hu, J. Yu and P. F. Barbara, *J. Phys. Chem. B*, 2001, **105**, 6103-6107.
84. L. Simine and P. J. Rossky, *J. Phys. Chem. Lett.*, 2017, **8**, 1752-1756.
85. W. Barford and O. R. Tozer, *J. Chem. Phys.*, 2014, **141**, 164103.
86. J. H. Bombile, M. J. Janik and S. T. Milner, *Phys. Chem. Chem. Phys.*, 2016, **18**, 12521-12533.
87. E. M. Y. Lee, W. A. Tisdale and A. P. Willard, *J. Phys. Chem. B*, 2015, **119**, 9501-9509.
88. S. B. Darling and M. Sternberg, *J. Phys. Chem. B*, 2009, **113**, 6215-6218.
89. M. Sim, J. Shin, C. Shim, M. Kim, S. B. Jo, J.-H. Kim and K. Cho, *J. Phys. Chem. C*, 2014, **118**, 760-766.
90. J. L. Brédas, G. B. Street, B. Thémans and J. M. André, *J. Chem. Phys.*, 1985, **83**, 1323-1329.
91. T. M. Burke and M. D. McGehee, *Adv. Mater.*, 2014, **26**, 1923-1928.
92. D. W. Gehrig, I. A. Howard, S. Sweetnam, T. M. Burke, M. D. McGehee and F. Laquai, *Macromol. Rapid Commun.*, 2015, **36**, 1054-1060.
93. F. C. Jamieson, E. B. Domingo, T. McCarthy-Ward, M. Heeney, N. Stingelin and J. R. Durrant, *Chem. Sci.*, 2012, **3**, 485-492.
94. S. V. Kesava, Z. Fei, A. D. Rimshaw, C. Wang, A. Hexemer, J. B. Asbury, M. Heeney and E. D. Gomez, *Adv. Energy Mater.*, 2014, **4**, 1400116.
95. B. M. Savoie, A. Rao, A. A. Bakulin, S. Gelinas, B. Movaghar, R. H. Friend, T. J. Marks and M. A. Ratner, *J. Am. Chem. Soc.*, 2014, **136**, 2876-2884.

96. H. Utzat, S. D. Dimitrov, S. Wheeler, E. Collado-Fregoso, P. S. Tuladhar, B. C. Schroeder, I. McCulloch and J. R. Durrant, *J. Phys. Chem. C*, 2017, **121**, 9790-9801.
97. M. Rubinstein and R. H. Colby, *Polymer Physics*, OUP Oxford, New York, NY, USA, 2003.
98. L. Ye, H. Hu, M. Ghasemi, T. Wang, B. A. Collins, J.-H. Kim, K. Jiang, J. H. Carpenter, H. Li, Z. Li, T. McAfee, J. Zhao, X. Chen, J. L. Y. Lai, T. Ma, J.-L. Bredas, H. Yan and H. Ade, *Nat. Mater.*, 2018, DOI: 10.1038/s41563-017-0005-1.
99. S. Cho, B. S. Rolczynski, T. Xu, L. Yu and L. X. Chen, *J. Phys. Chem. B*, 2015, **119**, 7447-7456.
100. J.-S. Kim, R. H. Friend, I. Grizzi and J. H. Burroughes, *Appl. Phys. Lett.*, 2005, **87**, 023506.
101. I. Hwang and G. D. Scholes, *Chem. Mater.*, 2011, **23**, 610-620.
102. P. C. Hiemenz and T. P. Lodge, *Polymer Chemistry, Second Edition*, Taylor & Francis, Boca Raton, 2007.
103. K. G. Jespersen, W. J. D. Beenken, Y. Zaushitsyn, A. Yartsev, M. Andersson, T. Pullerits and V. Sundström, *J. Chem. Phys.*, 2004, **121**, 12613-12617.
104. B. S. Rolczynski, J. M. Szarko, H. J. Son, Y. Liang, L. Yu and L. X. Chen, *J. Am. Chem. Soc.*, 2012, **134**, 4142-4152.
105. Q. T. Zhang and J. M. Tour, *J. Am. Chem. Soc.*, 1998, **120**, 5355-5362.
106. X. Liu, Y. Sun, B. B. Y. Hsu, A. Lorbach, L. Qi, A. J. Heeger and G. C. Bazan, *J. Am. Chem. Soc.*, 2014, **136**, 5697-5708.
107. C. Risko, M. D. McGehee and J.-L. Bredas, *Chem. Sci.*, 2011, **2**, 1200-1218.
108. R. Tautz, E. Da Como, C. Wiebeler, G. Soavi, I. Dumsch, N. Fröhlich, G. Grancini, S. Allard, U. Scherf, G. Cerullo, S. Schumacher and J. Feldmann, *J. Am. Chem. Soc.*, 2013, **135**, 4282-4290.
109. B. Bernardo, D. Cheyns, B. Verreet, R. D. Schaller, B. P. Rand and N. C. Giebink, 2014, **5**, 3245.
110. S. Gélinas, A. Rao, A. Kumar, S. L. Smith, A. W. Chin, J. Clark, T. S. van der Poll, G. C. Bazan and R. H. Friend, *Science*, 2014, **343**, 512-516.
111. P. E. Hartnett, C. M. Mauck, M. A. Harris, R. M. Young, Y.-L. Wu, T. J. Marks and M. R. Wasielewski, *J. Am. Chem. Soc.*, 2017, **139**, 749-756.
112. S. W. Provencher, *Computer Physics Communications*, 1982, **27**, 213-227.
113. K. Rurack and M. Spieles, *Anal. Chem.*, 2011, **83**, 1232-1242.

Table of Contents Entry

Push-pull architecture decreases the required conjugation length to achieve efficient charge transfer and enables single-site exciton dissociation.